



Original Research Article

Use of central composite design and surface modeling for cadmium (ii) ions removal from aqueous environment using novel modified layer double hydroxide

Mohtaram Janighorban^a, Nahid Rasouli^{a,*}, Nasrin Sohrabi^a, Mehrorang Ghaedi^b

^a Department of Chemistry, Payame Noor University, P.O. Box 19395-3697, Tehran, Iran

^d Chemistry Department, Yasouj University, Yasouj 75918-74831, Iran

ARTICLE INFORMATION

Received: 17 July 2020

Received in revised: 20 September 2020

Accepted: 8 October 2020

Available online: 7 November 2020

DOI: 10.22034/ajgc.2021.118922

KEYWORDS

Layered double hydroxide

Cd²⁺ adsorption

Response surface methodology

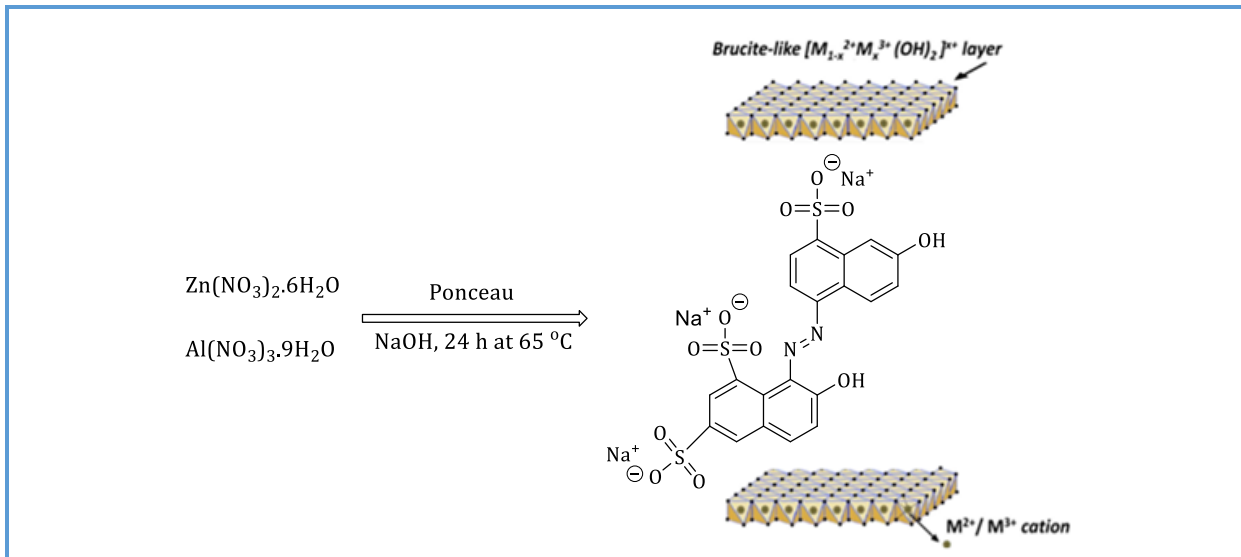
Central composite design

ABSTRACT

In this work, Zn₂Al-layered double hydroxide (LDH) that modified with Ponceau 4R (E 124) as food coloring, (Zn₂Al-LDH/Ponceau) was synthesized and characterized using different techniques including, X-ray diffraction analysis (XRD), Brunauer-Emmett-Teller (BET), field emission scanning electron microscopy (FE-SEM), and energy-dispersive X-ray (EDX) spectroscopy. Zn₂Al-LDH/Ponceau was then applied for Cd²⁺ removal from aqueous solution. The response surface methodology (RSM) approach using central composite design (CCD) was applied to develop a mathematical model and optimize process parameters for Cd²⁺ removal from aqueous solution using a chemically modified Zn₂Al-LDH/Ponceau. The optimal conditions to remove Cd²⁺ from aqueous solution were found to be initial Cd²⁺ concentration of 76 mg.L⁻¹, pH value of 4.22, adsorbed amount of 0.04 g, temperature of 30.3 °C, and the contact time of 46 min. The isotherm and kinetics and thermodynamics of the adsorption were investigated in detail. The obtained results suggested the adsorption of Cd²⁺ onto Zn₂Al-LDH/Ponceau follow Langmuir isotherm and the kinetic data are in good agreement with the Elovich kinetic model. In addition, the results of thermodynamic parameters indicated that the adsorption process was instantaneous nature and exothermic.

© 2021 by SPC (Sami Publishing Company), Asian Journal of Green Chemistry, Reproduction is permitted for noncommercial purposes.

Graphical Abstract

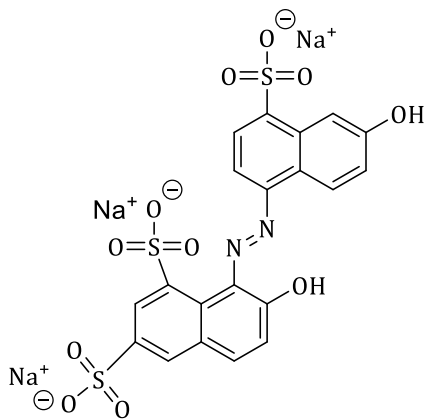


Introduction

Development of technology and its utilization has improved the entrance of heavy metals into the environment, lead to major environmental problems [1–5]. Heavy metal ions are highly toxic, non-biodegradable and can accumulate in the environment causing serious pollution in surface and groundwater. Accumulation of heavy metal ions in the living bodies can cause severe diseases, such as dementia, itai-itai disease, leukemia, and cancer [6–8]. So, the elimination of toxic metals from aqueous solution is a very significant process [9, 10]. Over the last few decades, some processes, including ion exchange, solvent extraction, bioremediation, limestone treatment, oxidation, chlorination, and ozonation followed by filtration have been used for iron removal from aqueous solution [11–16]. However, most of these approaches have high expenditure, average efficiency, generation of toxic secondary contamination, taking multiple time-consuming stages to completely process and inability to eliminate trace amounts of contaminants [17]. Among them, adsorption is

considered to be a more efficient process due to its economical and efficiency viewpoints. In fact, the adsorption technique is widely used for wastewater treatment because of its simplicity, ease of handling, high quality, low cost and excellent performance [18–24]. Recently, the advancement in nanotechnology suggested the promising future of nanomaterials for water treatment in an economical manner along with efficient adsorption capacities for heavy metal ions. Here, the layer double hydroxides (LDHs) become materials of choice due to its ease of functionalization, chemical accessibility, biocompatibility, non-toxicity, and attractive surface area. Hence, LDHs nanocomposites have been used as sorbents for heavy metals removal from aqueous solution. Layered double hydroxides (LDHs) known as the anionic clay have become well adsorbents due to their low cost, high surface area, highly flexible interior design [25], non-toxicity [26, 27], and anionic exchangeable properties [28]. Layered double hydroxide has the general formula as $[\text{M}_{1-\text{x}}^{\text{II}}\text{M}_{\text{x}}^{\text{III}}(\text{OH})_2]^{x+}[\text{A}_n]^{x/n}\text{mH}_2\text{O}$, where M^{II} , M^{III} and A_n which applied for a divalent, trivalent cation and the interlayer anion, such as CO_3^{2-} , Cl^- , NO_3^- .

and H₂O molecule, respectively. Layered double hydroxides have many applications such as super capacitors [29, 30], catalysis [31, 32], drug delivery [33, 34], wastewater management [35–38] and flame retardant epoxy formulation [39]. Earlier studies indicated that LDH intercalated with amino acids [40], ethylene diamine tetra acetic acid [41], diethylene tri-amine penta acetate and meso-2,3-dimercaptosuccinate [42], glutamate [43], possessed a higher affinity to potentially poisonous metal ions than the original LDH adsorbents. In this regard, LDHs have been modified in several methods to increase their adsorption ability [44, 45]. Therefore, an attempt has been made to enhance the adsorption capacity of these materials for removal of heavy metals [46, 47]. In this regard, Ponceau 4R (**Scheme 1**) was used for the modification of Zn₂Al-LDH to enhance the adsorption capacity of Zn₂Al-LDH for Cadmium ion adsorption.



Scheme 1. The Chemical structure of Ponceau 4R

Statistically designed experiments that investigate Cd²⁺ adsorption treatment systems have been conducted in a limited literature. To the best of our knowledge, there has been no study conducted on the synthesis of Ponceau 4R modification of Zn₂Al-LDH and using it as an

adsorbent for Cd²⁺ removal applying response surface methodology (RSM) modeling. Central composite design (CCD) is the most popular RSM approach. The RSM-CCD application possesses some advantages, such as experimental accuracy, minimization of experimental trials, and the amount of information gained for measuring goodness of fit.

Experimental

Materials and methods

All used materials were commercially reagents and purchased from the Merck and Fluka. Zinc (II) nitrate hexahydrate, Aluminium (III) nitrate ninehydrate, sodium hydroxide, Ponceau 4R and standard solution of titrosol cadmium were delivered from the Fluka and Merck. Cd²⁺ concentration was determined using atomic absorption spectrometer, Specter AA 220, VARIAN. Magnetic stirrer and water bath used were IKA, big-squid [ocean], and Julabo F12-MP, (from Germany), respectively. The study of the samples was examined by powder X-ray diffraction (Holland Philips X-pert, X-ray diffractometer with Cu-K α radiation). The particle size, external morphology, and analysis of elements were characterized using the scanning electron microscopy (SEM, model JEOL JEM-3010) and the BET analysis. The investigation of BET analysis was performed using the BELSORP Mini II instrument. A digital pH Burret 24, CRISON (PANIA) was employed for adjusting.

Preparation of Zn₂Al-LDH intercalated with ponceau

The Zn₂Al-layered double hydroxide (LDH) modified with Ponceau (Zn₂Al-LDH/Ponceau) was prepared usin a co-precipitation process [48]. In the first place, carbon dioxide free (CO₂-free) solution was accumulated by flowing N₂

into deionized water for 30 min at 60 °C, and used throughout the preparation process. In a typical procedure, a mixture of Zn(NO₃)₂.6H₂O (5.95 g, 0.02 mol) and Al(NO₃)₂.9H₂O (3.75 g, 0.01 mol) with Al to Zn molar ration (1:2) and Ponceau (12.09 g, 0.02 mol) in 250 mL deionized water was added to a solution of NaOH (1 M) at constant stirring speed up to reaching pH=10-11, then continue flowing N₂ in solution at 60 °C to complete precipitation procedure. The product obtained stirred at 65 °C for 24 h. The obtained solid product was dried at room temperature after several times filtration and washing with distilled water.

Adsorption studies

The concentrations of Cd²⁺ were calculated using the general typical flame atomic absorption spectrometry, at 228.8 nm wavelength, standard working concentration range: 0.25, 0.5, 1.0 and fuel acetylene. The efficiency of Cd²⁺ removal was calculated at different experimental conditions, according to CCD procedure. Adsorption potential for Cd²⁺ adsorption, isotherm studies at equilibrium with q_e (mg/g), kinetic study with q_t and thermodynamic study with q (mg/g), can be described by the following Equation 1.

$$q_e = \frac{(C_i - C_e)V}{m} \quad (1)$$

Where C_i and C_e (mg/L) refer to initial and equilibrium concentrations of cadmium, respectively, V (L) is the volume of cadmium solution, and m (g) is the mass of adsorbent.

In the kinetic studies, the Cd²⁺ adsorption amount (q_t) can be determined using the Equation 2.

$$q_t = \frac{(C_0 - C_t)}{C_0} \times 100 \quad (2)$$

Where C_i and C_t (mg/L) are concentration of Cd²⁺ at initial and time t, respectively, V (L) is

the volume of Cd²⁺ solution, and m (g) is the mass of Zn₂Al-LDH/Ponceau as an adsorbent.

Central composite design (CCD)

On the basis of statistical methods (depending on the problem under study), design of experiment identifies the effective parameters and decreases the uncontrollable variables. Response surface methodology (RSM) is one of the most common and widely used methods for experimental design. The RSM technique is a combination of statistical techniques for experimental modeling and process parameters optimization, in which a number of independent variables influence the desired response [49–52]. With this method, the number of experiments and all the coefficients of the quadratic regression model reduces and the interaction factors can be determined. In the RSM method, a model is specified for each independent variable through which the main interacting effects of the factors are expressed on each variable separately; the multivariate model is described as Equation 3 [53].

$$(Y)\% = \beta_0 + \sum_{i=1}^n \beta_i X_i + \sum_{i=1}^n \beta_i X_i^2 + \sum_{i=1}^{n-1} \sum_{j=2}^n \beta_{ij} X_i X_j + \varepsilon \quad (3)$$

Where Y is the predicted answer, β₀ is a constant coefficient, β₁, β₂, β₃ are linear effects, β₁₁, β₂₂, β₃₃ are square effects, β₁₂, β₁₃, β₂₃ are interacting effects and ε is the error of prediction equation. The central composite design (CCD) is one of the most widely used RSM methods [54–56] and is basically a two-level factorial approach in which central and axial points are introduced to allow for estimating the curvature of the model clearly. The RSM method with CCD design was used to optimize the adsorption process and evaluate the effects of independent variables on the response performance (the yield of heavy metal

removal). The effect of Cd²⁺ concentration (A), pH (B), adsorbent mass (C), contact time (D) and temperature bath (E) on adsorption yield

was optimized using five factors at 5 levels (- α , -1, 0, +1, + α) based on CCD in [Table 1](#).

Table 1. The levels of factors in CCD

Factors	Unit	Symbol	- α	levels				
				Low Actual	Mean	High Actual	+ α	Std.Dev.
Concentration(C)	mg.L ⁻¹	A	-1	35.00	57.500	80.00	+1	19.486
pH		B	-1	4.00	6.500	9.00	+1	2.165
adsorbent mass(m)	g	C	-1	0.027	0.046	0.064	+1	0.016
Contact time(time)	min	D	-1	35.00	60.00	85.00	+1	21.651
Temperature(T)	°C	E	-1	20.00	30.00	40.00	+1	8.660

Results and Discussion

Characterization of adsorbent

The XRD technique was used to identify the constituent phases of clays and also for investigation of structural changes after modifying. [Figure 1](#) indicates the XRD pattern of the Zn₂Al-LDH/Ponceau. The results revealed that the prepared Zn₂Al-LDH/Ponceau had the typical characteristics of the LDH phase ([Figure 1](#)) [57].

In the XRD pattern of Zn₂Al-LDH/Ponceau, the peaks are the same as Zn₂Al-LDH. Here, compared to Zn₂Al-LDH, the (003) diffraction peak of Zn₂Al-LDH/Ponceau shifts to the bigger 2 θ angle of 11.77 and the basal spacing decreased to 0.75 nm. The index of peaks in XRD patterns of Zn₂Al-LDH/Ponceau and Zn₂Al-LDH are depicted in [Table 2](#). This result can support intercalation of Ponceau in the Zn₂Al-LDH compound by the anion exchange process [58].

The crystallite sizes for the synthesized Zn₂Al-LDH/Ponceau were determined using Scherer formula [59] ([Equation 4](#)).

$$D = 0.9 \lambda / \beta \cos \theta \quad (4)$$

Where λ is the X-ray wavelength, β is full width at half maximum of the peak at various angle θ .

The estimated crystallite sizes were 32 nm. The morphology and chemical composition of the synthesized compounds were considered by FE-SEM and EDS, respectively. The FE-SEM images of the prepared samples are depicted in [Figure 2](#).

The primary sheet and lamellar structure of Zn₂Al-LDH modified after modification with Ponceau. The EDS spectrum of the prepared sample ([Figure 3](#)) demonstrates the presence of the relevant components, demonstrating purity of the synthesized Zn₂Al-LDH/Ponceau.

In the method of Brunauer-Emmett-Teller (BET) the physical adsorption of a vapor or gas onto the surface of a solid happened and the obtained data can be used to investigate the porosity of the compounds being studied. In this study, the BET method was used. The interference by the surrounding phase is difficult for the Bruner-Emmet-Teller (BET) N₂ adsorption/desorption isotherm method, because the surface is modified by vacuum action before N₂ adsorption process.

As seen in [Figure 4](#) and [Table 3](#), the Zn₂Al-LDH/Ponceau as adsorbent to posses great narrow micro-porosity. Also, the surface properties of the Zn₂Al-LDH as adsorbent are exhibited in [Table 3](#).

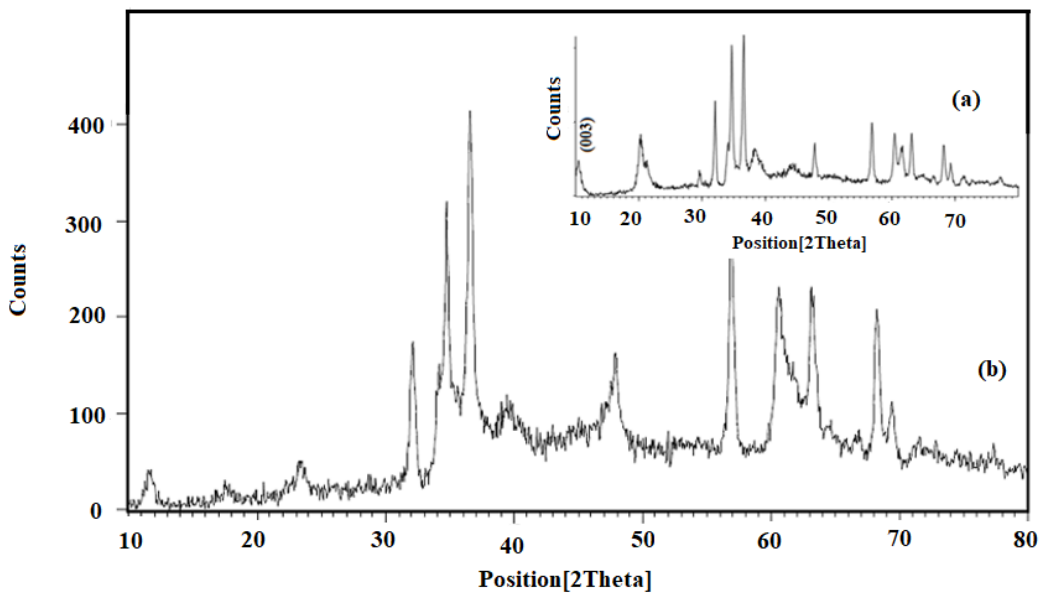
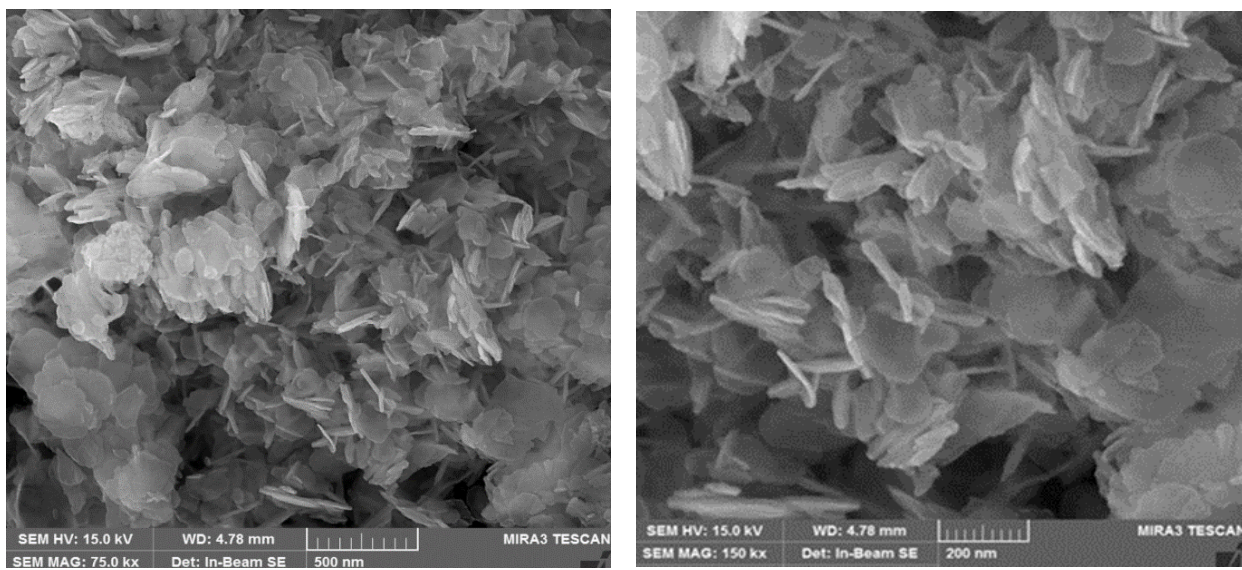


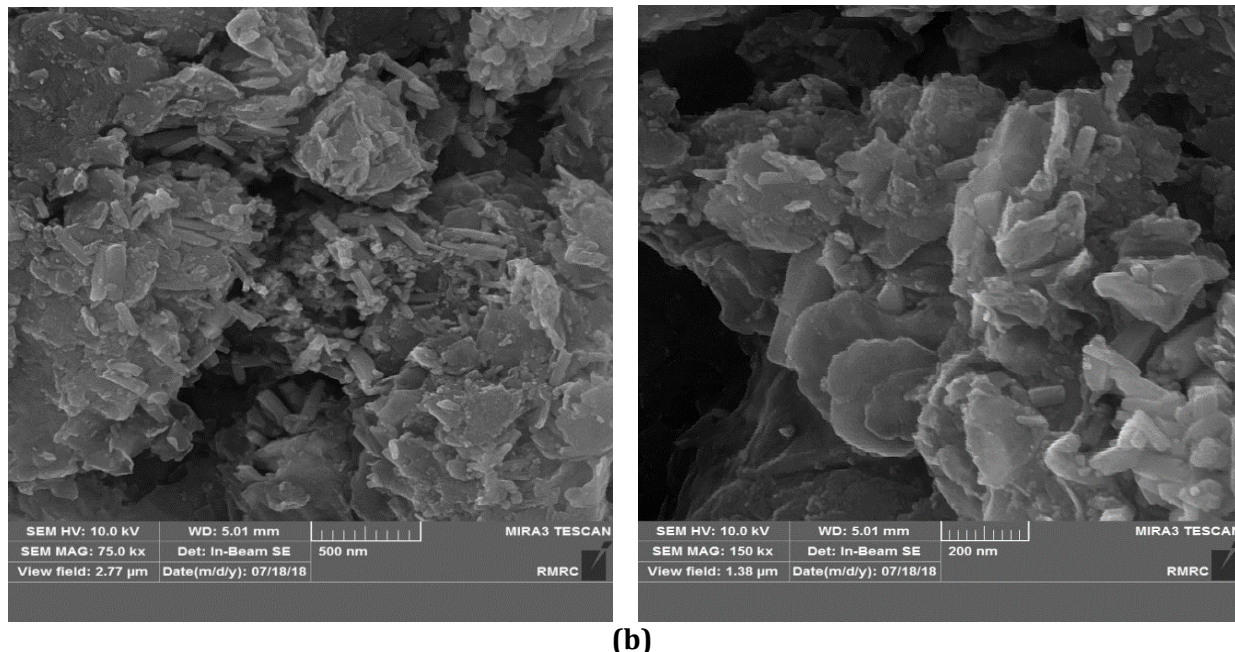
Figure 1. The XRD images of a) Zn₂Al-LDH and b) Zn₂Al-LDH/Ponceau

Table 2. The index of peaks in XRD patterns of Zn₂Al-LDH/Ponceau and Zn₂Al-LDH

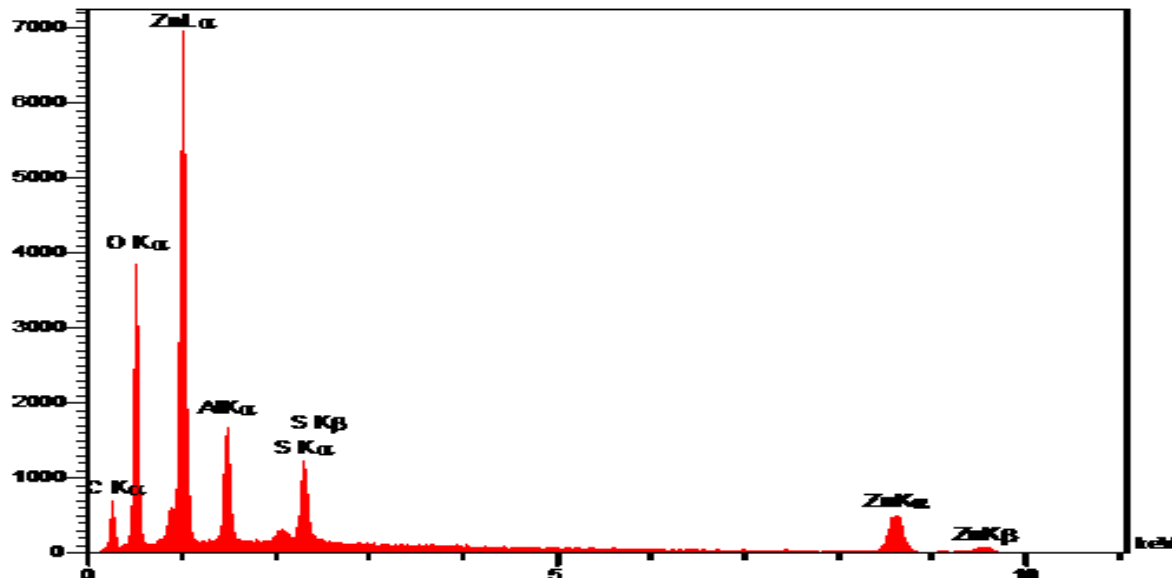
Zn ₂ Al-LDH/Ponceau	11.6575	17.6297	23.3867	32.1012	34.0644	34.7578	36.5722	39.4072
Zn ₂ Al-LDH	11.9830	-	23.7523	32.0144	-	34.7216	36.4855	39.4737
Zn ₂ Al-LDH/Ponceau	47.8340	-	59.9250	60.6383	63.1824	68.2410	694135	77.3524
Zn ₂ Al-LDH	47.8135	56.8188	-	60.4750	63.1172	68.2073	69.3494	77.2237



(a)



(b)

Figure 2. The FE-SEM images of a) Zn₂Al-LDH and b) Zn₂Al-LDH/Ponceau**Figure 3.** The EDS image of Zn₂Al-LDH/Ponceau

Design of experiment

In RSM method and CCD model, based on the defined experimental conditions, 32 different experiments were performed ([Table 4](#)) and the results were used to determine the optimal

conditions for removal of Cd²⁺ ions. By analysis of variance (ANOVA) using STATISTICA 10, the main variables and their influence on the response and their interactions with other variables were investigated.

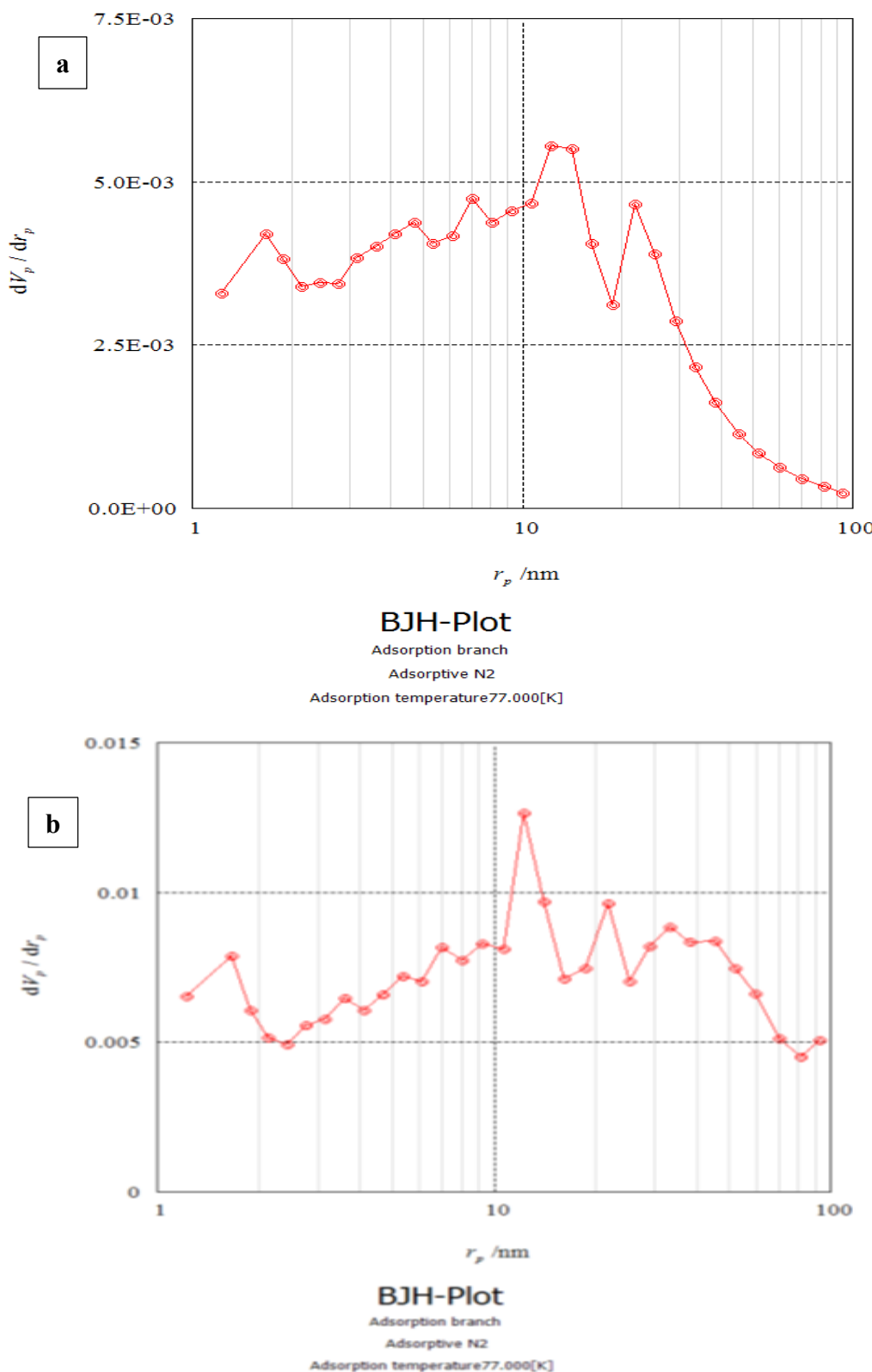


Figure 4. a) The BJH-Plot of $\text{Zn}_2\text{Al-LDH}/\text{Ponceau}$, b) The BJH-Plot of $\text{Zn}_2\text{Al-LDH}$

Table 3. Comparision between BJH-Plot of Zn₂Al-LDH/Ponceau and Zn₂Al-LDH

Sample	v _p (cm ³ /g)	a _p (m ² /g)	r _{p,Peak} (Area) (nm)
Zn ₂ Al-LDH/Ponceau	0.1733	30.510	12.20
Zn ₂ Al-LDH	0.6615	67.270	12.20

The results of, sum of squared (SS), degree of freedom (DF), the contribution of each parameter in the prediction model, the modified root sum squared, the average modified root sum squared, F-value and p-values are presented in the ANOVA tables. In statistics, the p-value indicates the probability value; the probability of the null hypothesis rejection is based on the correctness of this value with respect to the observed data [60]. The p-value can also determine the effect of a factor on a response [61], lower p-values correspond to higher importance of the model and the lower amount of p-values lower than 0.05 shows that the desired factor is important in the obtained results from this model [62]. In ANOVA, the F-value is the ratio of the mean regression sum of squares divided by the mean error sum of

squares; the more the F-value for an answer is, the more important is the effects of the considered levels of factors [63]. In this research study, with respect to the F-values and P-values the pH, concentration of metal ion (Con) and adsorbent dosage (Dose), time (t) and temperature (T) bath are the main parameters ([Table 5](#) and [Table 6](#)).

$$\begin{aligned} \text{\%Efficiency} = & 347.3711 - 3.1731 \times C - \\ & 11.3947 \times \text{pH} - 3214.1846 \times m - 2.1949 \times \\ & \text{time} - 5.0057 \times T + 0.1251 \times C \times \text{pH} + \\ & 11.478 \times C \times m + 8.0011 \times 10^{-3} \times C \times \text{time} - \\ & 0.0243 \times C \times T - 86.2092 \times \text{pH} \times m - \\ & 0.1102 \times \text{pH} \times \text{time} + 0.3817 \times \text{pH} \times T + \\ & 116372 \times m \times \text{time} - 6.8444 \times m \times T + \\ & 1.6975 \times 10^{-3} \times \text{time} \times T + 0.0163 \times C^2 + \\ & 0.6212 \times \text{pH}^2 + 31411.7815 \times m^2 + 0.0161 \times \\ & \text{time}^2 + 0.0726 \times T^2 \end{aligned} \quad (5)$$

Table 4. The matrix design and the responses

Run	A	B	C	D	E	%Efficiency	q _e
1	35	9	0.06	35	40	94	5.81
2	80	4	0.03	85	40	32.84	11.2
3	35	9	0.06	85	20	54.75	3.39
4	35	4	0.06	85	40	74.27	7.97
5	57.5	6.5	0.05	60	30	35.6	8.87
6	35	4	0.03	85	20	67.89	16.68
7	80	4	0.03	35	20	42.76	2.26
8	57.5	6.5	0.05	60	30	29.65	7.52
9	57.5	6.5	0.05	60	30	30.36	7.67
10	35	4	0.06	35	20	63.95	6.76
11	57.5	6.5	0.05	60	50	49.89	9.93
12	57.5	6.5	0.05	60	30	24.67	6.38
13	80	9	0.03	85	20	74.17	2.45
14	57.5	6.5	0.05	60	10	33.32	6.48
15	80	9	0.03	35	40	100	3.52
16	57.50	6.50	0.05	60	30	25.14	6.57
17	80	4	0.06	85	20	89.5	13.06
18	57.5	6.5	0.05	110	30	55.97	11.19
19	57.5	1.5	0.05	60	30	12.52	4.56

20	35	4	0.03	35	40	67.88	17.04
21	12.5	6.5	0.05	60	30	59.52	3.18
22	57.5	11.5	0.05	60	30	43.66	0.75
23	102.5	6.5	0.05	60	30	31.55	13.11
24	57.5	6.5	0.08	60	30	78.04	8.23
25	57.5	6.5	0.05	60	30	32.41	8.3
26	35	9	0.03	35	20	88.42	4.73
27	57.5	6.5	0.01	60	30	32.16	37.12
28	80	9	0.06	85	40	100	1.48
29	57.5	6.5	0.05	10	30	49.55	9.76
30	35	9	0.03	85	40	93	12.53
31	80	4	0.06	35	40	23.17	3.12
32	80	9	0.06	35	20	82.91	2.15

Table 5. The ANOVA results for the response 1, % efficiency, surface linear model

Source	Sum of Squares	df	Mean Square	F Value	p-value	
Model	17537.00	20	876.85	2.84	0.0393	significant
A-C	548.65	1	548.65	1.78	0.2093	
B-pH	3438.50	1	3438.50	11.14	0.0066	
C-m	480.17	1	480.17	1.56	0.2381	
D-time	54.51	1	54.51	0.18	0.6824	
E-T	121.28	1	121.28	0.39	0.5435	
AB	792.84	1	792.84	2.57	0.1372	
AC	361.29	1	361.29	1.17	0.3024	
AD	324.09	1	324.09	1.05	0.3274	
AE	478.19	1	478.19	1.55	0.2390	
BC	251.62	1	251.62	0.82	0.3859	
BD	758.31	1	758.31	2.46	0.1453	
BE	1457.14	1	1457.14	4.72	0.0525	
CD	458.50	1	458.50	1.49	0.2483	
CE	25.38	1	25.38	0.082	0.7796	
DE	2.88	1	2.88	9.338E-003	0.9248	
A^2	1993.37	1	1993.37	6.46	0.0274	
B^2	442.11	1	442.11	1.43	0.2565	
C^2	3317.55	1	3317.55	10.75	0.0073	
D^2	2962.61	1	2962.61	9.60	0.0101	
E^2	1546.53	1	1546.53	5.01	0.0468	
C^2	3317.55	1	3317.55	10.75	0.0073	
Residual	3394.18	11	308.56			
Lack of Fit	3305.52	6	550.92	31.07	0.0008	significant
Pure Error	88.66	5				
Cor Total	20931.18	31				

df: degrees of freedom

SS: the sum of the squared differences between the average values and the overall mean

Ms: mean squares, the sum of squares devided by df

SD: standard deviation

R²: R-Squared (coefficient of determination)

F-value: test for comparing term variance with residual (error) variance

Prob>F: the probability of seeing the observed F value if the null hypothesis is true

Residual: used to calculate the experimental error

Lack of fit: the data variation around the fitted model

Pure error: response variation in replicated design points

Cor total: totals of all information corrected for the mean

Table 6. Optimization Point of Zn₂Al-LDH/ Ponceau

C*,mg.L ⁻¹	pH*	m*,g	time*,min	T*, °C	Desirability	Selected
76	4.22	0.04	46	30.3	1.000	

Base on the results and Equation 5, the most important parameters on efficiency were Cd²⁺ concentration, temperature, amount of adsorbent, and pH.

Generally, when the coefficient of each parameter becomes high, it confirms a highly positive influence on the response. The negative value of each parameter indicates that there is a reverse correlation between responses and the parameter, meaning that the negative value results in the achievement of maximum responses [64]. According to this equation, Cd²⁺ concentration, pH, adsorbed amount, time and temperature bath have a negative effect on yield process (Cd²⁺ removal percentage). As is clear from this equation, the factors of C*pH, C*m, C*time, pH*T, m*time, time*T, C², pH², m², time² and T² have the most positive effect on the Cd²⁺ removal percentage; so, it means that with increasing of the factors, the Cd²⁺ removal yield increase. The factors of C*T, pH*m, pH*time and m*T have the most negative effect on Cd²⁺ removal percentage. Therefore, it by increasing the factors, the Cd²⁺ removal yield decrease.

Optimization of adsorption conditions

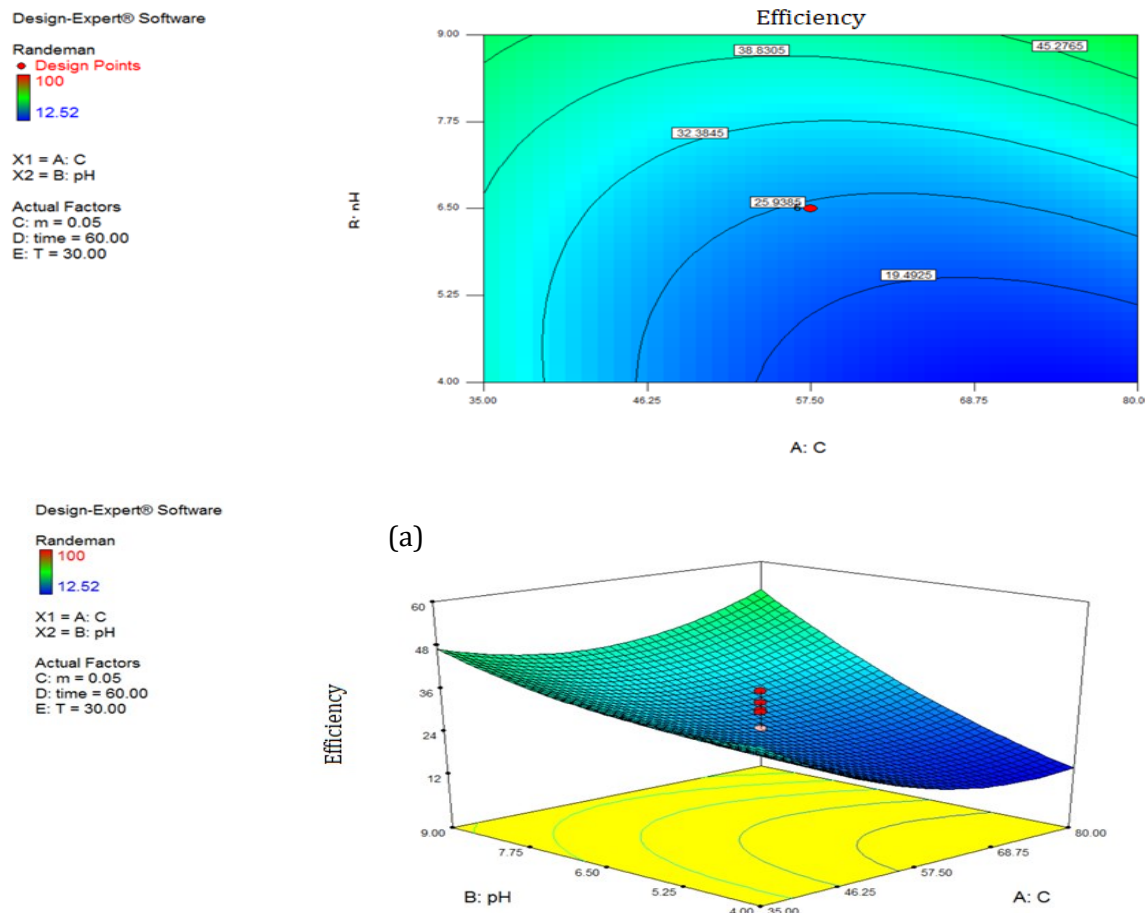
To optimize the critical factors and to describe the nature of the response surface, response surface methodology (RSM) along with CCD design are used [64]. Figure 5a–d demonstrates the relevant fitted response surfaces for the design and illustrates the

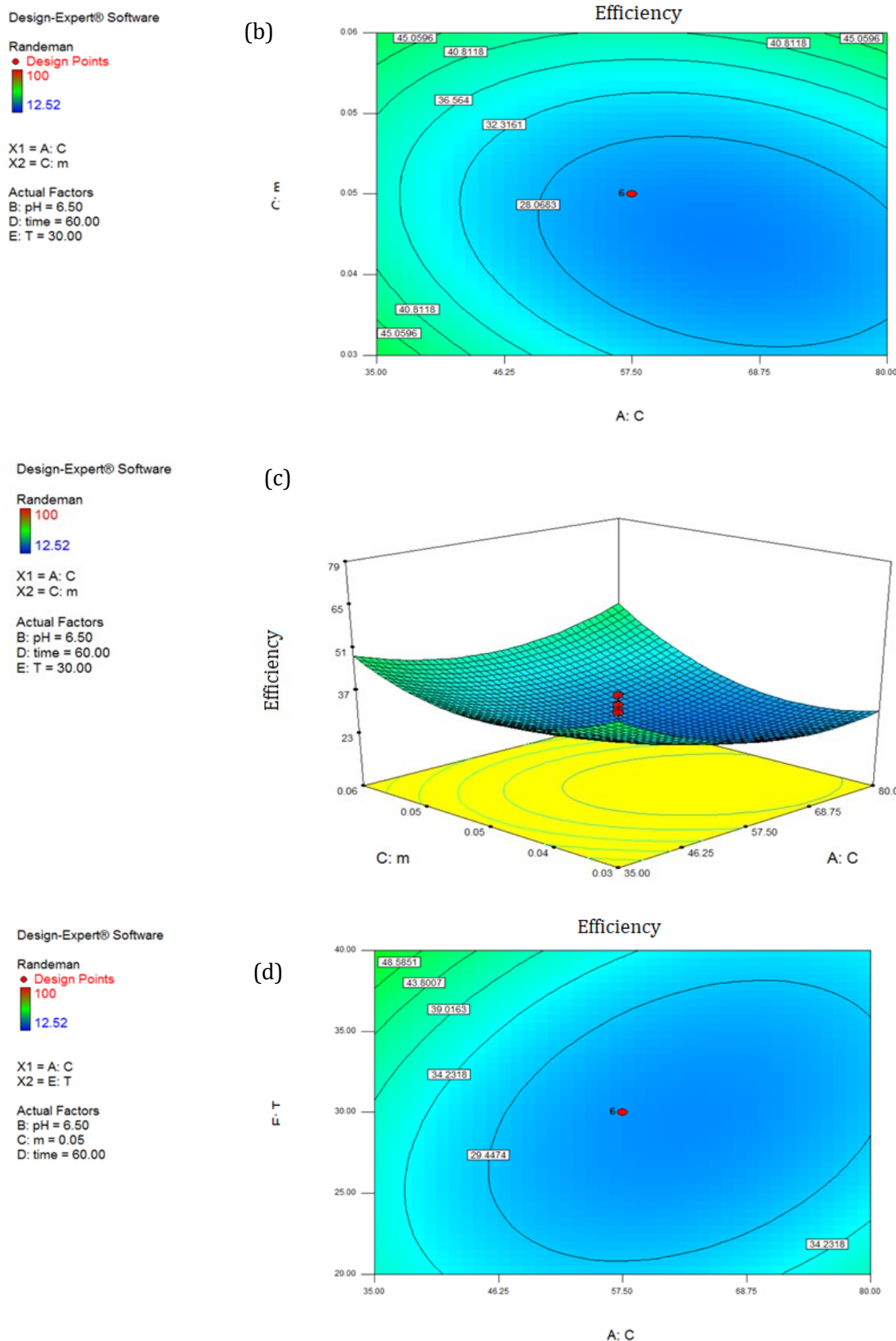
response surface plots of removal percent versus significant variables.

For a given pair of factors such plots were obtained at the center values of other variables. Graph curvatures show how the variables interact. The level of removal of Cd²⁺ has a very good interaction with mixing. The quick and rapid transfer of Cd²⁺ molecules to the adsorbent surface, which admit rapid balance, confirms the suitability and efficiency of mixing with magnetic stirrer as an effective wastewater treatment method. The results revealed that the initial adsorption rate is very fast due to the high available surface area and an adsorbent vacant site which enhances the interface and driving force. Adsorbent dosage interaction with other variables (Figure 5b) reveals a major correlation between percentages of Cd²⁺ removal at adsorbent dosage. Due to the high ratio of Cd²⁺ molecules to vacant site, the removal percentage decreased significantly at a lower amount of adsorbent. Figure 5a and 5b demonstrate the association of pH with the initial Cd²⁺ concentration and dosage of adsorption, respectively. The percentage of elimination of Zn₂Al-LDH /Ponceau slowly increases by increasing the pH. This result is due to the fact that protonation is caused at low pH. High repulsive forces between the cationic Cd²⁺ molecules and the adsorbent therefore contribute to a decrease in the percentage of removal of Cd²⁺. Above pH of 6, the Cd²⁺ ion precipitates in water as hydroxide. The rise in the initial pH, thus leads to less decrease in the

percentage of Cd²⁺ elimination. Figure 5a and 5c indicate the influence of the initial concentration of Cd²⁺ and its interaction with other influences. It was found that given the rise in the amount of Cd²⁺ concentration, its removal efficiency has been reduced and at lower concentrations of Cd²⁺, the ratio of solvent concentrations to adsorbent sites is lower, resulting in an increase in the removal of Cd²⁺ ions. At the higher concentrations, the lower adsorption yield is due to the saturation of adsorption sites. On the other hand, at medium initial Cd²⁺ concentrations, the percentage removal of Cd²⁺ was higher and lower at higher initial concentrations, which clearly shows that the adsorption of Cd²⁺ from its aqueous solution depended on its initial concentration. The STATISTICA 7.0 program uses the profile for expected values and the desirable method to

optimize the variable influences (Figure 5). Profiling the desirability of the responses requires defining the DF by assigning expected values for each dependent variable (removal per cent). The individual desirability scores are used to measure the percentage of elimination, and the desirability of 1.0 has been selected as the goal value, as shown in Table 4. The basis of these measurements and desirability score of 1.0 was obtained at optimum conditions set as (Table 5) an initial concentration Cd²⁺ of 76 mg L⁻¹, a pH value of 4.22, adsorbent amount of 0.04 g, temperature of 30.3 °C and contact time of 46 min. The triplicate conduction of similar experiments at the optimized value of all parameters has RSD% less than 3% and are strongly correlated with the obtained data using CCD design.





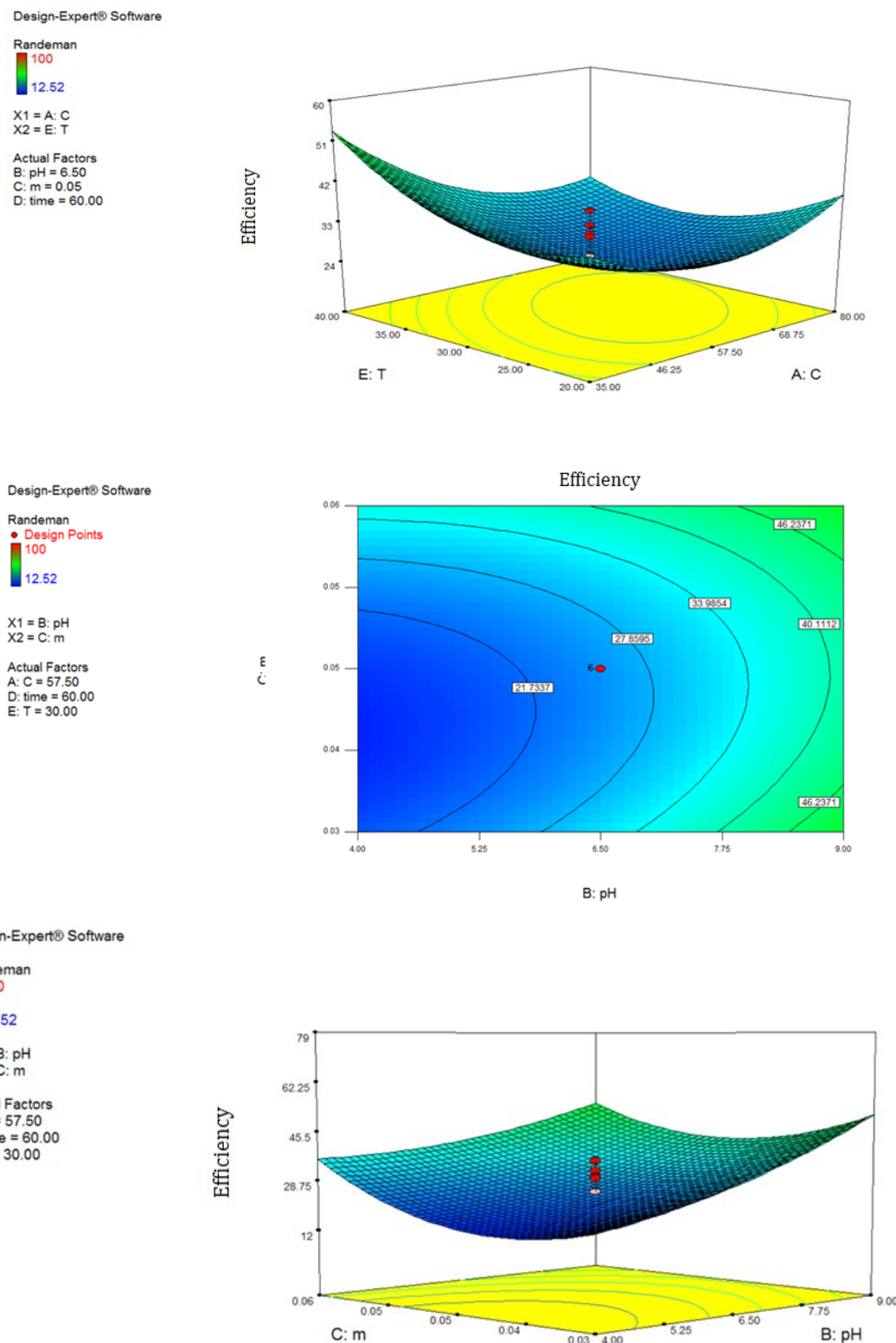


Figure 5a-d. The 3D surfaces and contour plots for interactive effect variables

Equilibrium isotherms models

The isothermal equilibrium adsorption is used to provide valuable information about the mechanism, properties and tendency of adsorbent toward Cd²⁺. In other words, adsorption isotherms exhibit the extent and mechanism of the process which is proportional to surface properties which simply estimated fitting experimental equilibrium data to different models such as Langmuir, Freundlich and Tempkin. According to our previous reports and based on their linear form, slopes and intercepts respective constants are estimated [65]. Also, experimental results based on the higher values of correlation coefficients ($R^2 \sim 1$) indicated reasonable applicability of Langmuir model for Cd²⁺ adsorption onto Zn₂Al-LDH /Ponceau. The experimental results from adsorption of Cd²⁺ by Zn₂Al-LDH /Ponceau were analyzed by Langmuir, Freundlich and Temkin models. The Langmuir isotherm equation can be defined as Equation 6 [66].

$$\frac{C_e}{q_e} = \frac{1}{q_{\max}} K_L + \frac{C_e}{q_{\max}} \quad (6)$$

Where q_e (mg g⁻¹) and C_e (mg g⁻¹) are the amounts of adsorbed dye per unit mass of adsorbent and unadsorbed dye concentration in solution at equilibrium time, respectively, q_{\max}

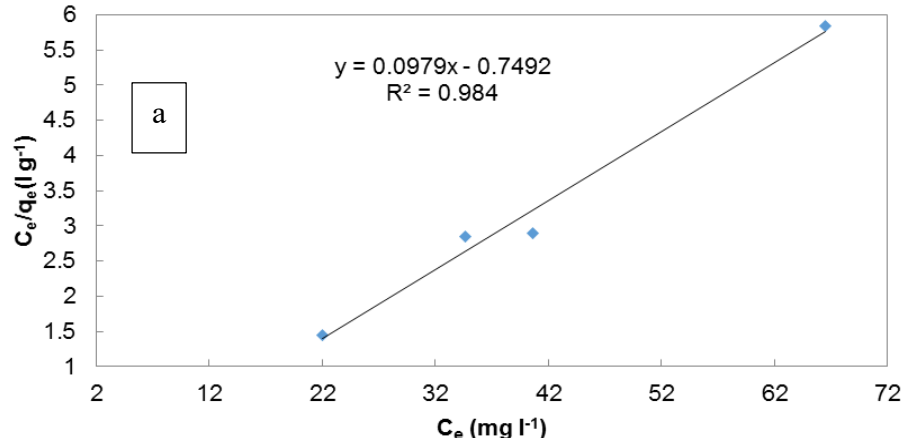
is the maximum amount of the Amaranth dye per unit mass of adsorbed on the surface bound at high C_e (mg g⁻¹), and K_L is adsorption equilibrium constant (Lmg⁻¹). Figure 6a depicts the linear plot of C_e/q_e vs. C_e of Langmuir isotherm. The values of q_{\max} and K_L were calculated from the slope and intercepts of the plots and are presented in Table 7. The Freundlich's adsorption isotherm model can be used for a multilayer heterogeneous adsorption and expressed as Equation 7 [67].

$$\log q_e = \frac{1}{n} \log C_e + \log K_F \quad (7)$$

Where q constants are correlated to the maximum adsorption capacity and n is the adsorption intensity. Figure 6b indicates the linear plot of ($\log q_e$ vs. $\log C_e$) of Freundlich isotherm. The plot of $\log q_e$ vs. $\log C_e$ was applied to give the intercept value of K_F and the slope of $1/n_F$. The heat of the adsorption and the interaction of adsorbent adsorbate were studied using Tempkin isotherm model as expressed in Eq. (8) [68]:

$$q_e = \beta_T \ln K_T + \beta_T \ln C_e \quad (8)$$

In this model, B_t is the Tempkin constant related to the heat of adsorption (J.mol⁻¹), T is the absolute temperature (K), and K_T is the equilibrium binding constant (L.mg⁻¹). Figure 6c exhibits the linear plot of q_e vs. $\ln C_e$ of Tempkin isotherm model.



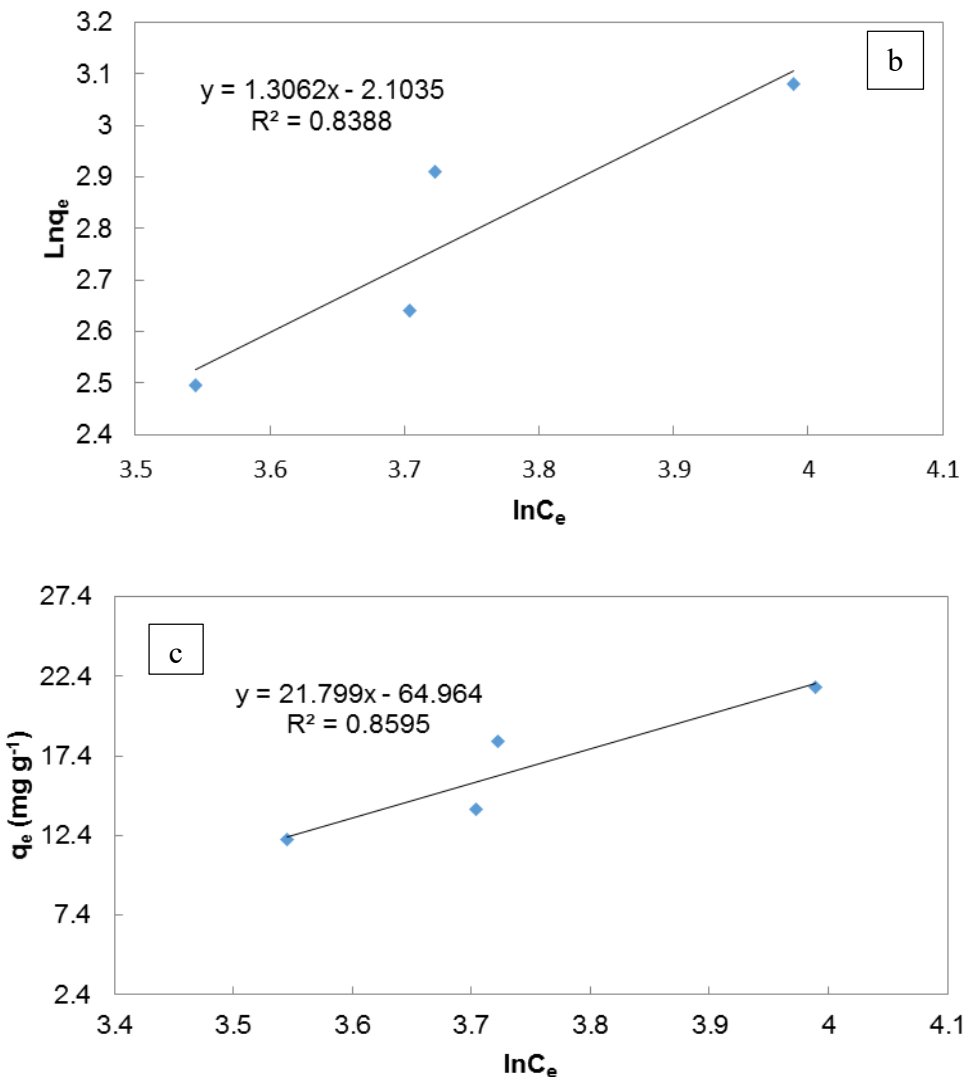


Figure 6. The plot of a) Langmuir equilibrium isotherm, b) Frundlich isotherm and c) Tempkin isotherm, experimental conditions ($C=46, 56, 66, 76, 86, 96$ and 106 mg L^{-1} , $\text{pH}=4.22$, $m=0.04 \text{ g}$, $T=30.3 \text{ }^\circ\text{C}$, $t=46 \text{ min}$)

Table 7. Isotherm constant parameters and correlation coefficients based on adsorption of Cd^{2+} onto $\text{Zn}_2\text{Al-LDH}/\text{Ponceau}$

Isotherm	Equation	Parameters	Value
Langmuir	$\frac{C_e}{q_e} = \frac{1}{K_L q_m} + \frac{C_e}{q_m}$	$q_m (\text{mg g}^{-1})$	10.2145
		$K_L (\text{L mg}^{-1})$	-0.1307
		R^2	0.984
Freundlich	$\ln q_e = \ln K_F + \frac{1}{n} \ln C_e$	n	0.7656
		$K_F (\text{L mg}^{-1})$	0.1182
		R^2	0.8388
Temkin	$q_e = \beta_T \ln K_T + \beta_T \ln C_e$	B_T	21.799
		$K_T (\text{L mg}^{-1})$	0.0508
		R^2	0.8595

Table 7 summarizes the constant parameters of isotherm equations and the correlation coefficient (R^2) for isotherm models. The strong correlation of coefficient at various conditions for analyzing of the experimental data indicates the applicability of Tempkin model.

Adsorption kinetics

The kinetic research can provide useful insights regarding the reaction mechanisms, and the adsorption mechanism is a surface phenomenon arising from the binding forces

between the adsorbent atoms, molecules and ions and the adsorbent surface [69]. Specific kinetic models are used to monitor the mechanisms of the adsorption processes such as mass transfer and chemical reactions [70]. From this study, the rate of adsorption (as a factor in efficiency of adsorbent) and the mechanism of adsorption can be concluded. Adsorption kinetics of Cd^{2+} was evaluated using various models including, pseudo-first-order, pseudo-second order, intra particle diffusion, and Elovich models (39 Lin Deng).The various parameters were estimated from the plots of the kinetic model equations (**Table 8**).

Table 8. Kinetic parameters for Cd^{2+} removal onto $Zn_2Al-LDH/Ponceau$

Model	Equation	Parameters	Value
Pseudo-first-order	$\ln(q_e - q_t) = \ln q_e - K_1 t$	$K_1 (\text{min}^{-1})$	-0.09
Pseudo-second-order	$\frac{t}{q_t} = \frac{1}{k_2 q_e^2} + \left(\frac{1}{q_e}\right) t$	$k_2 (\text{g mg}^{-1} \text{ min}^{-1})$ q_e R^2	0.0376 -23.4192 0.9909
Intra particle diffusion	$q_t = K_{id} t^{\frac{1}{2}} + C$	K_{id} C R^2	3.4525 -4.0329 0.9901
Elovich	$q_t = \frac{1}{\beta} \ln(\alpha\beta) + \frac{1}{\beta} \ln(t)$	α β R^2	1.3175 0.0835 0.9931

All the kinetic equations are shown in **Table 8**, where k_1 and k_2 ($\text{g mg}^{-1} \text{ min}^{-1}$) are the pseudo-first-order and pseudo-second-order rate constants for adsorption and R^2 is the correlation coefficient to express the uniformity between the predicted and experimental data. The parameter of α ($\text{mg.g}^{-1} \text{ min}^{-2}$) is the initial adsorption rate and β ($\text{g.mg}^{-1} \text{ min}^{-1}$) is the desorption constant related to the extent of surface coverage and activation energy for chemisorption process. All of the investigated models were fitted by a linear regression to the experimental data, evaluating their appropriateness based on the corresponding

correlation coefficients R^2 . The correlation coefficient (R^2) and agreement between the experimental and calculated values of q_e , are the criteria for applicability of each model. Good agreement between two q_e values and the high values of ($R^2 \sim 1$) show that the adsorption follows the Elovich kinetic model (**Table 8**).

It is clear that the correlation coefficients for the Elovich model ($R^2 \sim 0.9930$) are higher than for the pseudo-second order ($R^2=0.9909$) and the models for intraparticle diffusion ($R^2=0.9903$), suggesting that the current system can be well described in the adsorption phase by the Elovich kinetic model (**Table 9**). The

highest R^2 value of this model (1.0000) confirms the applicability of this model to interpret the experimental data. From all the correlation coefficients, it can be deduced that the Elovich kinetic model is the most suitable model for Cd^{2+} adsorption, indicating that the adsorption process is mainly controlled by chemical adsorption and ion exchange and surface

adsorption mechanism occur in the adsorption process. As seen in Figure 7d, the plots of q_t versus $\ln(t)$ indicate a relatively good linear correlation, suggesting that the Elovich equation is useful to describe the chemical adsorption, ion exchange and surface adsorption mechanism process.

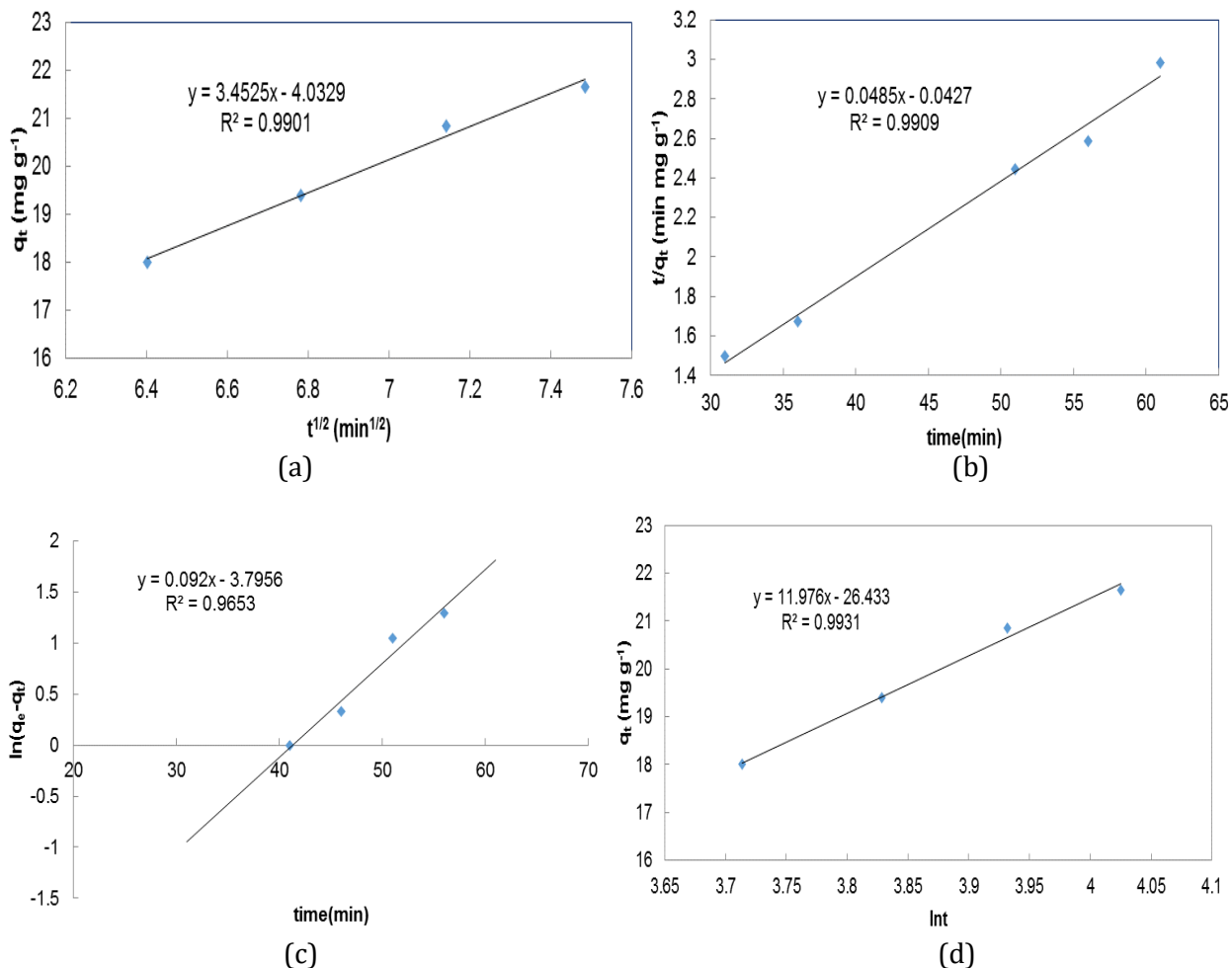


Figure 7. The plot of a) pseudo- first- order b) pseudo -second-order c) intra particle diffusion and d) Elovich , experimental conditions ($C=76 \text{ mg.L}^{-1}$, $\text{pH}=4.22$, $m=0.04 \text{ g}$, $T= 30.3^\circ\text{C}$, $t = 31, 36, 41, 46, 51, 56$ and 61 min)

Thermodynamic study

Thermodynamic analysis of an adsorption is dispensable to deduce if the process happens spontaneously or not, and provide information

about internal energy changes that are associated with that. The Gibbs free energy (ΔG°), enthalpy change (ΔH°), and entropy

change (ΔS°) are obtained using the following Equations [70].

$$\Delta G^\circ = -RT \ln K_c \quad (9)$$

$$\ln K_c = \frac{\Delta S^\circ}{R} - \frac{\Delta H^\circ}{RT} \quad (10)$$

Where K_c is the solid-liquid distribution coefficient that can be calculated by the intercept of plot of $\ln(q_e/C_e)$ vs. q_e , R is the universal gas constant ($8.314 \text{ J mol}^{-1}\text{K}^{-1}$) and T is the absolute temperature. The plots of $\ln K_c$ vs. $1/T$ give the straight line from which ΔH°

and ΔS° are determined from the slope and intercept, respectively (Figure 8).

Table 9 summarized the obtained ΔG° , ΔH° and ΔS° . The positive value of ΔG° ($250.003 \text{ J mol}^{-1}$) shows that the unfeasible and non spontaneous. The negative value of ΔH° ($-1.2762 \text{ J mol}^{-1}$) indicates that the adsorption process is exothermic. Also, the negative value of ΔS° ($-0.8281 \text{ J mol}^{-1} \text{ K}^{-1}$) also suggests decreased freedom at the solid-solution interface during Cd^{2+} adsorption on the active sites of $\text{Zn}_2\text{Al-LDH}/\text{Ponceau}$.

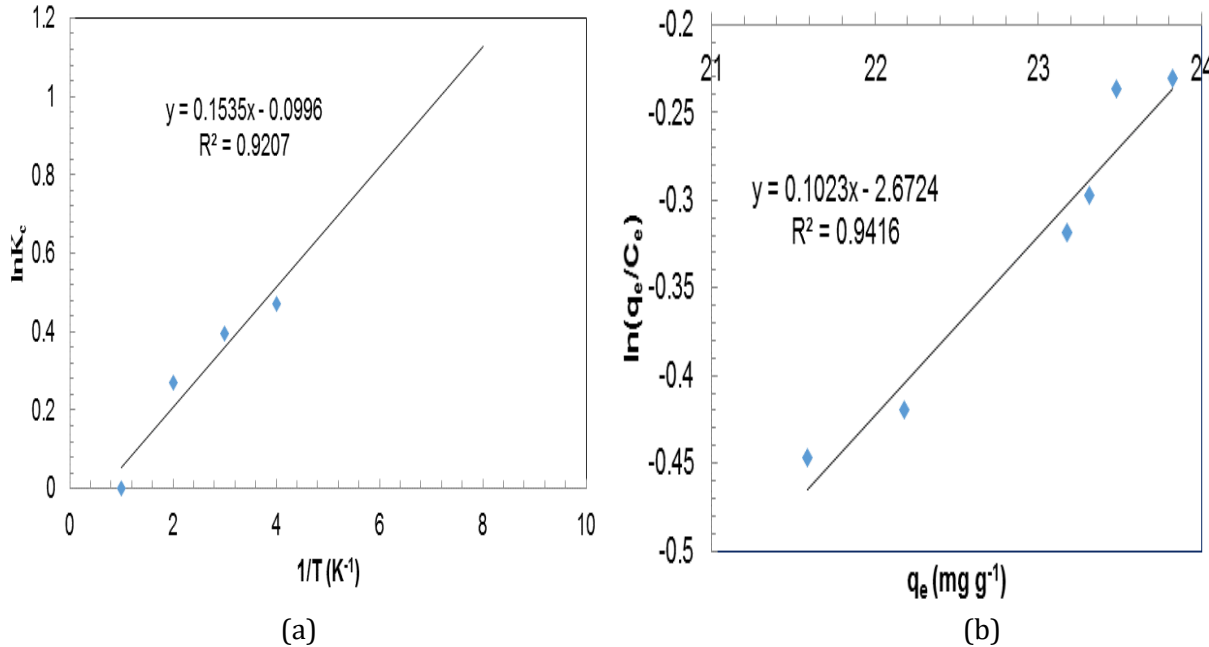


Figure 8. The Vant Hoff plots of $\text{Zn}_2\text{Al-LDH}/\text{Ponceau}$ for determining of (a) ΔG° , (b) ΔH° and ΔS° , experimental conditions ($C=76 \text{ mg L}^{-1}$, $\text{pH}=4.22$, $m=0.04 \text{ g}$, $T=15.3, 20.3, 25.3, 30.3, 35.3, 40.3, 45.3 \text{ }^\circ\text{C}$, $t=46 \text{ min}$)

Table 9. The thermodynamic parameters for Cd^{2+} adsorption onto $\text{Zn}_2\text{Al-LDH}/\text{Ponceau}$

Parameters	$\Delta H^\circ (\text{J mol}^{-1})$	$\Delta S^\circ (\text{J mol}^{-1} \text{ K}^{-1})$	$\Delta G^\circ (\text{J mol}^{-1})$	$\ln K_c$	R^2
	-1.2762	-0.8281	250.003	0.983	0.9207

Reusability of the $\text{Zn}_2\text{Al-LDH}/\text{ponceau}$

The reusability of the adsorbent for further use is a key feature for evaluation its performance [71]. The ability of reusing the

adsorbents in several successive separation processes was examined. The results demonstrated that, the $\text{Zn}_2\text{Al-LDH}/\text{Ponceau}$ can be reused for five times without any decrease in their efficiency (Figure 9).

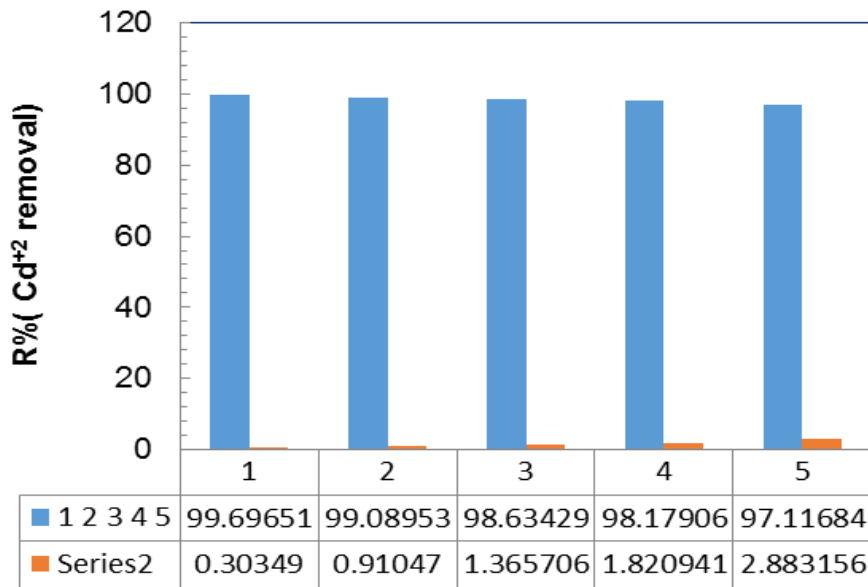


Figure 9. The ability of reusing Zn₂Al-LDH/Ponceau in five successive separation processes

Zero point charge determination

To evaluate the zero point charge (pHz) of Zn₂Al-LDH/Ponceau, 0.1 M NaCl was prepared, and its initial pH was adjusted between 4.0 and 11.0 using HCl and NaOH. Then, 20 mL of 0.1 M NaCl was taken in 25 mL flasks and 0.036 g Zn₂Al-LDH/Ponceau was added to each solution. These flasks were kept for 24 h and the

final pH of the solutions was measured with a pH meter. Graphs were plotted between final pH and initial pH. As seen in [Figure 10](#), at 7.485, $\Delta\text{pH}=0$, therefore, the pHz=7.485. The adsorption studies for adsorption of Cd²⁺ was carried out at pH=7.4 based on the zeta potential analysis of the Zn₂Al-LDH//Ponceau as adsorbent which has been previously discussed.

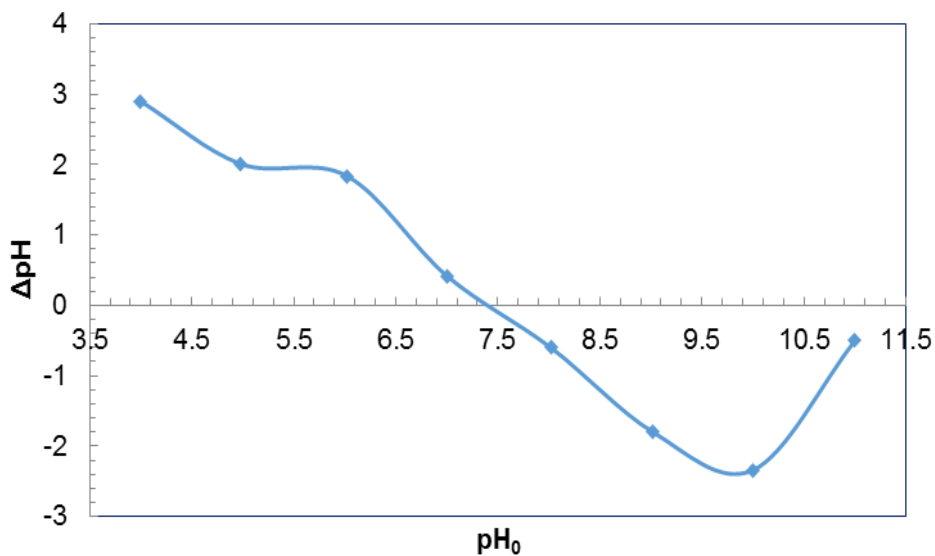


Figure 10. Zero point charge determination

Thus, the adsorption of the ions such as Pb^{2+} , Cd^{2+} ions in the adsorbent may be attributed to the interaction of the species that are dominant at $\text{pH}<8$, such as Pb^{2+} , Cd^{2+} , $\text{Pb}(\text{OH})^+$ and $\text{Cd}(\text{OH})^+$ with the functional groups on the surface of adsorbent (active hydroxyl groups on the $\text{Zn}_2\text{Al-LDH}$) [72]. So, metal ions which can interact with the functional groups on the adsorbent increase the probability of metal ion

removal. Thus, due to the multiple-ion-binding sites on the adsorbent surfaces and the metal ion species a number of metal-adsorbent complexes are formed during adsorption process [73]. In this work, a comparison of the Cd^{2+} removal efficiency by the $\text{Zn}_2\text{Al-LDH}/\text{Ponceau}$ and other adsorbents in new literature was shown in Table 10.

Table 10. Comparison of adsorption capacities of various adsorbents for Cd^{2+} removal from aqueous solution

Adsorbent	q_{\max} (mg.g^{-1})	Ref.
FeMnMg-LDH	59.99	
Nano hydroxyapatite	9.8	[52]
$\text{NH}_2\text{-MCM-41}$	18.25	[53]
MgAl-Humate-LDH	39.2	[54]
MgAl-Cl-LDH	71.15	[55]
MgAl-H100-LDH	53.95	
MgAl-H50-LDH	27.79	
MgAl-edta-LDH	17	[56]
MgAl-CO ₃ -LDH	1	
ZnAl-DTPA-LDH	44.8	[57]
ZnAl-DSMA-LDH	112	
ZnAl-NO ₃ -LDH	3.02	
ZnAl-edta-LDH	42.15	[58]
MgAl-CO ₃ -LDH	61.4	[59]
$\text{Fe}_3\text{O}_4/\text{MgAl-CO}_3\text{-LDH}$	45.6	
Clinoptilolite	4.88	[60]
Tourmaline	33.11	[61]
$\text{Zn}_2\text{Al-LDH}/\text{Ponceau}$	10.2145	this work

Application of $\text{Zn}_2\text{Al-LDH}/\text{P}$ in real sample

To evaluate the applicability of the optimized adsorption method, the synthesized adsorbent $\text{Zn}_2\text{Al-LDH}/\text{P}$ was used for the removal of Cd^{2+} from seawater collected from Battery factories as a real sample. Table 11, illustrates the experimental conditions and the obtained analytical results as well as percentage removal efficiencies and adsorption capacity.

Also, in order to show the effects of interfering of other heavy metal ions with the action of $\text{Zn}_2\text{Al-LDH}/\text{P}$ in adsorbing Cd^{2+} , we performed more experiments on the real

sample. The elements in Table 12 were found in the battery unit wastewater sample that was reported by ICP analysis.

Table 12 and 13 exhibits the analytical results before adsorption and after adsorption as well as percentage removal efficiencies. In the presence of these cationic disturbances as well as severe anionic sulfate disturbance in the effluent, Cd^{2+} adsorption was carried out and the results displayed that amount of Cd^{2+} ions was increased by 137.5 to 152%, and by correction and based on the recovery, the adsorption values were applied to calculate the value of q_e and %R.

Table 11. Application of Zn₂Al-LDH/P for removal of Cd²⁺ in real sample

Run	Wast water cc	Concentration of Cd ²⁺ (mg/L)	pH	adsorbent, (g)	T(°C)	Time (min)	%R	q _e (mg/g)
1	50	0	4.22	0.04	30.3	46	30.7826	0.3715
2	50	1	4.22	0.04	30.3	46	6.31604	0.077
3	50	2	4.22	0.04	30.3	46	5.6607	0.0992
4	50	3	4.22	0.04	30.3	46	9.4344	0.225
5	50	4	4.22	0.04	30.3	46	7.6957	0.2128
6	50	5	4.22	0.04	30.3	46	3.5442	0.1129

Table 12. Application of Zn₂Al-LDH/P for investigation of interfering of other heavy metal ions in the real sample

Run	Element	C(mg/L)	Run	Element	C(mg/L)
1	As	0.009	14	Co	0.08
2	Cd	1.97	15	Li	0.11
3	Se	0.09	16	Mn	1.25
4	Pb	3.56	17	Ti	0.21
5	Cr	7.06	18	Zn	1.44
6	Fe	48.1	19	Bi	<0.1
7	Mo	0.39	20	Sr	20.8
8	Sn	2.82	21	Ni	5.59
9	Sb	0.25	22	W	<0.1
10	Al	4.58	23	Pd	<0.002
11	V	0.03	24	Na	843
12	Ba	0.05	25	Si	0.58
13	Cu	0.51	26	K	67.4

Table 13. Application of Zn₂Al-LDH/P for removal of Cd²⁺ in real sample after adsorption

Run	Wast Water (cc)	Concentration of Cd ²⁺ (mg/L)	pH	Adsorbent (g)	T(°C)	Time (min)	%R	q _e (mg/g)	% Recovery
1	50	0	4.22	0.04	30.3	46	30.7826	0.3715	-
2	50	1	4.22	0.04	30.3	46	6.31604	0.077	83.9
3	50	2	4.22	0.04	30.3	46	5.6607	0.0992	86.7
4	50	3	4.22	0.04	30.3	46	9.4344	0.225	139.3
5	50	4	4.22	0.04	30.3	46	7.6957	0.2128	129.275
6	50	5	4.22	0.04	30.3	46	3.5442	0.1129	129.42

Conclusions

A central composite design is the most common response surface design, and it builds on a factorial design; it just adds center points and star (axial) points, effectively transforming

your "cube" of inference into a fully rotatable, symmetric star. The central composite design created significantly better models compared to the other methods. As the central composite design requires a smaller number of experiments, its models were used for

theoretical examination of experimental space. CCD designs provide high quality predictions over the entire design space, but require factor settings outside the range of the factors in the factorial part. When the possibility of running a CCD design is recognized before starting a factorial experiment, factor spacings can be reduced to ensure that $\pm \alpha$ for each coded factor corresponds to reasonable levels. A Central Composite Design requires five factorial levels. Box-Behnken Designs (BBD) use the midpoints of the cube edges instead of the corner points, which results in fewer runs, but, unlike the Central Composite Design, you have to do all the runs; you can't stop in the middle, even if there is no curvature. The Box-Behnken Design uses only three factor levels, and should be used when your screening experiment indicated curvature is probably significant. BBD requires fewer treatment combinations than a central composite design in cases involving 3 or 4 factors. The Box-Behnken design is rotatable (or nearly so); however, it contains regions of poor prediction quality. BBD have less design points when compare to axial points of CCD hence no of experiments are more in CCD compared to BBD. CCD also tests at extreme conditions and hence this gives better for quadratic models. CCD will require more experiments (20 experiments for 3 factors) as compared to BBD (15 experiments for 3 factors). BBD is more nearer to the face centered composite design ($\alpha=1$) but with fewer experiments. For CCD However $\alpha=\sqrt{\text{number of experiments}}$. Plackett-Burman design (PBD) is not suitable for optimization. The purpose of using PBD is to determine the most significant factors (Screen design). In general, Plackett-Burman is not recommended because interactions are partially confounded or "aliased" with main effects. This study indicates the Zn₂Al-LDH/Ponceau potential as an effective

adsorbent used to removal Cd²⁺ from wastewater. CCD was used to monitor the effects of parameters on the removal efficiency of Cd²⁺ ions. The optimized conditions for maximum Cd²⁺ adsorption were an initial concentration of Cd²⁺ of 76 mg/L, pH value of 4.22, adsorbent dose of 0.04 g/L, the temperature of 30.3 °C, and contact time of 46 min. The experimental results obtained from aqueous solutions for the adsorption of Cd²⁺ ions have been checked with isotherm equations and illustrated that Langmuir isotherm is more compatible than the others. Additionally, the kinetic data matched very well with the Elovich kinetic model. Also, thermodynamic experiments indicated that the process of adsorption was uns spontaneous and exothermic.

Acknowledgement

The financial support of the research council of Payame Noor University of Isfahan is gratefully acknowledged.

Disclosure Statement

No potential conflict of interest was reported by the authors.

References

- [1]. Jalilian M., Shahmari A., Taheri K., Gholami K. *Ultrason Sonochem.*, 2020, **61**:104802
- [2]. Abdollahi F., Taheri A., Shahmari M. *Sep Sci & Technol.*, 2020, **55**:2758
- [3]. Thacker H., Ram V., Dave P.N. *Prog. Chem. Biochem. Res.*, 2019, **2**:84
- [4]. Bader N., Elmajbry A., Al borki Z., Ahmida A., Geath A. *Prog. Chem. Biochem. Res.*, 2020, **3**:1
- [5]. Ambarak M., Asweisi A. *Adv. J. Chem. B.*, 2020, **2**:10

- [6]. Dey P., Gola D., Mishra A., Malik A., Singh D.K., Patel N., Von Bergen M., Jehmlich N. *J. Hazard. Mater.*, 2016, **318**:679
- [7]. Monisha J., Tenzin T., Naresh A., Blessy BM., Krishnamurthy N.B. *Interdiscip. Toxicol.*, 2014, **7**:60
- [8]. Jarup L. *Br. Med. Bull.*, 2003, **68**:167
- [9]. Farasati M., Haghghi S., Boroun S. *Desalin. Water Treat.*, 2016, **57**:11162
- [10]. Sheng J., Qiu W., Xu B., Xu H., Tang C. *Environ. Sci. Pollut. Res.*, 2016, **23**:11034
- [11]. Mohammadnezhad G., Dinari M., Soltani R. *New J. Chem.*, 2016, **40**:3612
- [12]. Cui H., Fan Y., Yang J., Xu L., Zhou J., Zhu Z. *Chemosphere*, 2016, **161**:233
- [13]. Dinari M., Soltani R., Mohammadnezhad G. *J. Chem. Eng. Data.*, 2017, **62**:2316
- [14]. Lee C.G., Park J.A., Choi J.W., Ko S.O., Lee, S.H. *Water Air Soil Pollut.*, 2016, **227**:456
- [15]. Li M., Gong Y., Lyu A., Liu Y., Zhang H. *Appl. Surf. Sci.*, 2016, **383**:133
- [16]. Mohammadnezhad G., Abad S., Soltani R., Dinari M. *Ultrason. Sonochem.*, 2017, **39**:765
- [17]. Visa M., Chelaru A.M. *Appl. Surf. Sci.*, 2014, **303**:14
- [18]. Yang K., Yan L.G., Yang Y.M., Yu S.J., Shan R.R., Yu H.Q., Zhu B.C., Du B. *Sep. Purif. Technol.*, 2014, **124**:36
- [19]. Ahmadi F., Esmaeili H. *Desalin water treat.*, 2018, **110**:154
- [20]. Foroutan R., Mohammadi R., Farjadfar S., Esmaeili H., Saberi M., Sahebi S., Dobaradaran S., Ramavandi B. *Environ Sci Pollut Res Int.*, 2019, **26**:6336
- [21]. Khoshkerdar I., Esmaeili H. *Acta Chimica Slovenica*, 2019, **66**:208
- [22]. Foroutana F., Esmaeilib H., Sanatic A.M., Ahmadid M., Ramavandif B. *Desalin water treat.*, 2018, **135**:236
- [23]. Ramezani F., Zare-Dorabei R. *Polyhedron*, 2019, **166**:153
- [24]. Kiani A., Haratipour P., Ahmadi M., Zare-Dorabi R., Mahmoodi A. *J Water Supply Res T.*, 2017, **66**:239
- [25]. Yao W., Yu S., Wang J., Zou Y., Lu S., Ai Y., Alharbi N.S., Alsaedi A., Hayat T., Wang X. *Chem. Eng. J.*, 2017, **307**:476
- [26]. Becker C.M., Gabbardo A.D., Wypych F., Amico S.C. *Compos Part A Appl. Sci. Manuf.*, 2011, **42**:196
- [27]. Gu Z., Atherton J.J., Xu Z.P. *Chem. Commun.*, 2015, **51**:3024
- [28]. Carretero M.I. *Appl. Clay. Sci.*, 2002, **21**:155
- [29]. Das J., Das D., Parida K.M. *J. Colloid Interface Sci.*, 2006, **301**:569
- [30]. Cai X., Shen X., Ma L., Ji Z., Xu C., Yuan A. *Chem. Eng. J.*, 2015, **268**:251
- [31]. Nishimura Sh., Takagaki A., Ebitani K. *Green Chem.*, 2013, **15**:2026
- [32]. Li C., Wei M., Evans D.G., Duan X. *Small.*, 2014, **10**:4469
- [33]. Ladewig K., Xu Z.P., Lu G.Q. *Exp. Opin. Drug. Deliv.*, 2009, **6**:907
- [34]. Kim M.H., Park D.H., Yang J.H., Choy Y.B., Choy J.H. *Int. J. Pharm.*, 2013, **444**:120
- [35]. Das J., Patra, B.S., Baliarsingh N., Parida K.M. *Appl. Clay. Sci.*, 2006, **32**:252
- [36]. Goh K.H., Lim T.T., Dong Z. *Water. Res.*, 2008, **42**:1343
- [37]. Bharali D., Deka R.C. *Colloids Surf. A.*, 2017, **525**:64
- [38]. Abdellaoui K., Pavlovic I., Bouhent M., Benhamou A., Barriga C. *Appl. Clay. Sci.*, 2017, **134**:142
- [39]. Dos Santos R.M., Gonçalves R.G., Constantino V.R., Santilli C.V., Borges P.D., Tronto J., Pinto, F.G. *Appl. Clay. Sci.*, 2017, **140**:132
- [40]. Bharali D., Deka R.C. *Colloids Surf. A.*, 2017, **525**:64
- [41]. Tran H.N., Lin C.C., Chao H.P. *Sep. Purif. Technol.*, 2018, **192**:36

- [42]. Pérez M.R., Pavlovic I., Barriga C., Cornejo J., Hermosín M.C., Ulibarri, M.A. *Appl. Clay Sci.*, 2006, **32**:245
- [43]. Yanming S., Dongbin L., Shifeng L., Lihui F., Shuai C., Haque M.A. *Arab. J. Chem.*, 2017, **10**:10
- [44]. Ahmed I.M., Gasser M.S. *Appl. Surf. Sci.*, 2012, **259**:650
- [45]. Drici N., Setti N., Jouini Z., Derriche Z. *J. Phys. Chem. Solids.*, 2010, **71**:556
- [46]. Pavlovic I., Pérez M.R., Barriga C., Ulibarri M.A. *Appl. Clay Sci.*, 2009, **43**:125
- [47]. Liang S., Guo X.Y., Feng N.C., Tian Q.H. *J. Hazard. Mater.*, 2010, **174**:756
- [48]. Deng L., Zhou Si., Wang Li., Zhou Sh. *J Phys Chem Solids.*, 2017, **104**:79
- [49]. Mousavi J., Parvini M. *Int J Hydrogen Energy.*, 2016, **41**:5188
- [50]. Chatterjee S., Kumar A., Basu S., Dutta S. *Chem Eng J.*, 2012, **181**:289
- [51]. Amini M., Younesi H., Bahramifar N. *Chemosphere.*, 2009, **75**:1483
- [52]. Vaezi M., Vishlaghi M.B., Tabriz M.F., Moradi O.M. *J Alloys Compd.*, 2015, **635**:118
- [53]. Marchitan N., Cojocaru C., Mereuta A., Duca G., Cretescu I., Gonta M. *Sep Purif Technol.*, 2010, **75**:273
- [54]. Bhatti M.S., Reddy A.S., Kalia R.K., Thukral A.K. *Desalination.*, 2011, **269**:157
- [55]. Bajpai S. *J Hazard Mater.*, 2012, **227**: 436
- [56]. Sarkar M., Majumdar P. *Chem Eng J.*, 2011, **175**:376
- [57]. Sun Y., Zhou J., Cheng Y., Yu J., Cai W. *Adsorpt. Sci. Technol.*, 2014, **32**:351
- [58]. Xu J., Song Y., Tan Q., Jiang L. *J Mater Sci.*, 2017, **52**:5908
- [59]. Langford J., Wilson A. *J. Applied Crystallography.*, 1978, **11**:102
- [60]. Mousavi J., Parvini M. *Int J Hydrogen Energy.*, 2016, **41**:5188
- [61]. Kumar M.S., Phanikumar B. *Environ Sci Pollut Res.*, 2013, **20**:1327
- [62]. Bhatti M.S., Reddy A.S., Kalia R.K., Thukral A.K. *Desalination.*, 2011, **269**:157
- [63]. Bajpai S.J. *Hazard Mater.*, 2012, **227**:436
- [64]. Adinarayana K., Ellaiah P. *J. Pharm. Pharmaceut. Sci.*, 2002, **5**:272
- [65]. Liu Q.X., Zhou Y.R., Wang M. *Adsorpt Sci Technol.*, 2019, **37**:312
- [66]. Citak D., Tuzen M., Soylak M. *Food and Chem. Toxicol.*, 2009, **47**:2302
- [67]. Khairul Anwar M.S., Nor Zakirah I., Ramizah Liyana J., Nurul Ain M.A., Norsuzailina M.S., Genevieve G., Rubiyah B., Nur Syuhada A.Z. *Int. J. Eng. Tech.*, 2018, **7**:91
- [68]. Koohzad E., Jafari D., Esmaeili H. *Chem Select.*, 2019, **4**:12356
- [69]. Foroutan R., Mohammadi R., Farjadfar S., Esmaeili H., Ramavandi B., Sorial G.A. *Adv Powder Technol.*, 2019, **30**:2188
- [70]. Nandi B.K., Goswami A., Purkait M.K. *J. Hazard. Mater.*, 2009, **161**:387
- [71]. Fazelirad H., Taher M.A. *Environ. Technol.*, 2015, **37**:300
- [72]. Kikuchi Y., Qian Q., Machida M., Tatsumoto H. *Carbon.*, 2006, **44**:195
- [73]. Akpomie K.G., Dawodu F.A., Kayode O., Adebowale K.O. *Alex. Eng. J.*, 2015, **54**:757

How to cite this manuscript: Mohtaram Janighorban, Nahid Rasouli*, Nasrin Sohrabi, Mehrorang Ghaedi. Use of central composite design and surface modeling for cadmium (ii) ions removal from aqueous environment using novel modified layer double hydroxide. *Asian Journal of Green Chemistry*, 5(2) 2021, 151-175. DOI: 10.22034/ajgc.2021.118922